Ordered Phases in Rod−Coil Diblock Copolymers

M. Müller* and M. Schick

Department of Physics, Box 351560, University of Washington, Seattle, Washington 98195-1560

Received May 30, 1996; Revised Manuscript Received August 27, 1996[⊗]

ABSTRACT: We study spatially ordered phases in a rod−coil diblock copolymer melt. In the weak segregation limit, we solve the self-consistent field equations by a partial numerical evaluation of the single chain partition function. In the strong segregation limit, we resort to a brushlike approximation. The structural asymmetry of the blocks has a pronounced influence on the phase diagram. We find that the only stable morphologies are those in which the coils are on the convex side of the rod−coil interface. The results are compared to experiment.

I. Introduction

The self-assembly of diblock copolymers has attracted a great deal of interest for basic, theoretical reasons as well as technological ones. The chemical joining of two distinct homopolymers into a diblock copolymer prevents macrophase separation of the two pieces and leads instead to the appearance of spatially ordered structures. The particular periodic superstructure which forms balances the free energy costs of the interfaces between unlike blocks, which favors long wavelength periodic units, and the entropy loss due to chain stretching, which favors shorter ones.[1]

In many practical applications the blocks of the copolymer are characterized by some degree of structural asymmetry. For example, a flexible block may be chosen as it contributes to the composite material a resistance to fracture and may be joined to a more rigid portion which contributes tensile strength[2] or possesses favorable dielectric properties. The orientational order and electrical conductance of a constituent block can be exploited in optical[3] and electrical devices.[4,5]

The influence of the stiffness on the phase behavior of binary homopolymer blends has attracted much theoretical interest,[6−9] but there is much less work on copolymer systems and their spatially ordered phases. In the strong segregation limit, Semenov and Vasilenko[10] examined such phases of a rod−coil system with strong, anisotropic interactions. Assuming that the rods are strictly aligned in the direction normal to the lamellae, they predict a transition from a monolayer to a bilayer lamellar phase. Halperin[11] investigated the transition between a smectic A structure, in which the rods are aligned perpendicular to the layers, and a smectic C, in which they are tilted. A phase of disklike micelles is also found to be stable.[12] In the weak segregation limit, only spatially uniform phases of diblocks had been examined[13] until recently. Matsen[14] has now studied the effect on the diblock lamellar phases of varying stiffness, while Netz and Schick[15] have examined the result of introducing anisotropic interactions between the semiflexible blocks and also of subjecting them to external fields. Only lamellar structures have been investigated, however.

In this paper we highlight the influence of the disparity of stiffness between blocks on microphase separation by consideration of rod−coil copolymers. Anisotropic interactions between rods are ignored so that the effect of their stiffness is manifest only in a reduction in their entropy and via a local incompressibility constraint. We apply self-consistent field theory, but in contrast to refs 14 and 15, we calculate single chain partition functions via partial enumeration.[16] The scheme is formulated for arbitrary architecture but applied to the rod−coil system in the weak segregation limit. The results are compared to the phase diagram in the strong segregation limit and to experiment.

II. Numerical Self-Consistent Field Theory

The partition function of an incompressible system comprising n AB copolymers can be written in the form

$$Z \sim \int \Pi_{\alpha=1}^{n} D[r_\alpha] P[r_\alpha] \delta[1 - \hat{\phi}_A - \hat{\phi}_B] \times \exp\{-\rho_0^2 \int dr\, dr'\, \hat{\phi}_A(r) V_{AB}(r - r') \hat{\phi}_B(r')\} \quad (2.1)$$

where $1/\rho_0$ denotes the segmental volume, V_{AB} the mutual, segmental interaction between dissimilar blocks, and $P[r]$ the probability distribution characterizing the noninteracting, single chain conformations. We do not include anisotropic interactions. The dimensionless monomer density takes the form

$$\hat{\phi}_A(r) = \frac{1}{\rho_0} \sum_{\alpha=1}^{n} \sum_{i_A} \delta(r - r_{\alpha,i_A}) \quad (2.2)$$

where the sum runs over all A-monomers in copolymer α. A similar expression holds for $\hat{\phi}_B(r)$. Employing a Hubbard-Stratonovich transformation, we rewrite the many chain partition function in terms of a single particle problem in external, fluctuating fields W_A, and W_B:

$$Z \sim \int D\Phi_A D W_A D W_B \exp\left\{-\frac{F}{k_B T}\right\} \quad (2.3)$$

where the free energy functional is defined by

$$\frac{F[\Phi_A, W_A, W_B]}{n k_B T} = -\ln Q + \frac{\rho_0 N}{V} \int dr\, dr'\, \Phi_A(r) V_{AB}(r - r')(1 - \Phi_A(r')) - \frac{1}{V} \int dr\, (W_A \Phi_A + W_B(1 - \Phi_A)) \quad (2.4)$$

and Q denotes the single chain partition function in the

[⊗] Abstract published in *Advance ACS Abstracts,* November 15, 1996.

S0024-9297(96)00782-6 CCC: $12.00

fields W_A and W_B:

$$Q = \int D[r]P[r] \exp\{-\sum_{i_A} W_A(r_{i_A})/N - \sum_{i_B} W_B(r_{i_B})/N\} \tag{2.5}$$

The leading contribution to the partition function (2.3) stems from those values ϕ_A, w_A, and w_B of the collective variables Φ_A, W_A, and W_B, which extremize the free energy functional, and the mean-field approximation consists of retaining only this contribution. The values are determined by the self-consistent equations:

$$\phi_A(r) + \phi_B(r) = 1$$

$$w_A(r) - w_B(r) = - \int dr' \, N \, \rho_0 V_{AB}(r - r')(\phi_A(r') - \phi_B(r'))$$

$$\phi_A(r) = -\frac{V}{Q}\frac{\delta Q}{\delta w_A(r)} \quad \text{and} \quad \phi_B(r) = -\frac{V}{Q}\frac{\delta Q}{\delta w_B(r)} \tag{2.6}$$

The mean field approximation reduces the original problem of mutually interacting chains to one of a single chain in a static, external field which is determined self-consistently. Composition fluctuations are neglected, but the coupling between chain conformations and composition is not. In order to study the self-assembly into different morphologies, we expand the fields and densities which occur in the above equations in a complete set of orthonormal functions,[17] $\{f_k\}$, which possess the symmetry of the phase being considered; $\phi_A = \sum_k \phi_{A,k} f_k$, $w_A = \sum_k w_{A,k} f_k$, and $w_B = \sum_k w_{B,k} f_k$.

Rather than solving the single chain problem analytically,[14,15] we evaluate the single chain partition function Q numerically,[16] employing a representative sample of p single chain conformations which obey the distribution P. Giving each polymer conformation a weight,

$$w_c = \exp\{-\sum_k (w_{A,k} \sum_{i_A} f_k(r_{c,i_A})/N + w_{B,k} \sum_{i_B} f_k(r_{c,i_B})/N)\} \tag{2.7}$$

we obtain the following expressions for the partition function and the A monomer density:

$$Q = \frac{1}{p}\sum_{c=1}^{p} w_c \quad \text{and} \quad \phi_{A,k} = \frac{\sum_{c=1}^{p} w_c \sum_{iA} f_k(r_{c,i_A})/N}{\sum_{c=1}^{p} w_c} \tag{2.8}$$

A similar expression is obtained for ϕ_B. The resulting set of nonlinear equations is solved by a Newton−Raphson-like method.

This scheme is applicable to arbitrary chain architectures, and one can use conformational data extracted from experiments or simulations as input. We apply it to rod−coil diblock copolymers consisting of $N = 50$ segments, of which fN segments are modeled as a rigid rod of length fbN with $b = 1$, and the remaining $(1 - f)N$ segments are modeled as connected via Gaussian springs of length $a = 1$. The segmental interaction is taken to be of the simple form $V_{AB}(r - r') = \delta(r - r')\chi/\rho_0$. In order to evaluate the single chain partition function, we employ up to 200 000 single chain conformations and up to 32 basis functions. This is sufficient to determine the phase boundaries in the weak segregation limit, as presented in Figure 1. In agreement with previous calculations[13] employing the random phase approximation, the ordered phase is more stable than in coil−coil diblock copolymers, and the phase diagram is slightly asymmetric in the copolymer composition f. Most notably, only phases in which the coils are on the convex side of the red−coil interface are found to be thermodynamically stable. This result emphasizes the importance of the conformational entropy of the flexible component which is increased when the coil occupies the larger space on the convex side of the interface.

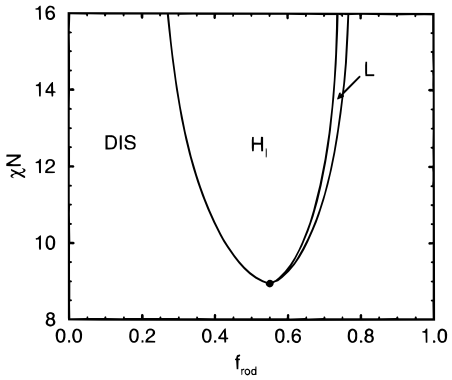

Figure 1. Mean field phase diagram of a rod−coil copolymer melt in the weak segregation limit, using the numerical evaluation of the single chain partition function. $a = b = 1$.

III. Strong Segregation Theory

At higher incompatibility, the chain stretching and the sharpening of the interfaces require an increase in the number of chain conformations and basis functions to be used in the above procedure, which eventually exceeds our computational facilities. In the strong segregation limit, we resort to a brushlike approximation[1,18] to determine the phase boundaries. In the limit of large incompatibility, the interface between the rod-rich and coil-rich regions is much smaller than the spatial extension R of the unit cell, and the free energy is determined by a competition of the interfacial free energy F_{inter} and the stretching cost F_{conf} of the coil-like portion. We assume that the rigid part of the copolymer fills the space without free energy costs[19] and neglect the translational entropy of the junctions between rod and coil at the interface[10] and the entropy associated with the distribution of chain ends.[20] The free energy contribution per chain can be cast in the form

$$\frac{F_{inter}}{nk_BT} = c_1\frac{\gamma N}{\rho_0 R} \quad \text{and} \quad \frac{F_{conf}}{nk_BT} = c_2\frac{R^2}{Na^2} \tag{3.1}$$

where the surface tension is γk_BT and the constants c_1 and c_2 characterize the different morphologies. On approximation of the hexagonal or cubic unit cells by cylindrical or spherical ones of radius R,[18] one obtains for these constants the values compiled in Table 1. Minimization of the free energy with respect to the unit cell size R yields

$$R_{opt}^3 = \frac{c_1 N^2 \gamma a^2}{2c_2\rho_0} \quad \text{and} \quad \frac{F_{min}}{nk_BT} = 3\left(\frac{c_1^2 c_2 \gamma^2 N}{4a^2\rho_0^2}\right)^{1/3} \tag{3.2}$$

The strong stretching assumption is valid as long as the chains are not completely extended. Therefore, the condition $R_{opt} \ll N$ or $(\gamma/N) \ll 1$ must be fulfilled. The free energies of the different morphologies are presented in Figure 2.

Since cylindrical and spherical unit cells cannot fill space,[18] the above result is a lower bound for the free

Table 1. Coefficients in the Strong Stretching Approximation (Eq 3.1) for the Different Morphologies

	lamellar L	inverted hexagonal H_I rod inside	hexagonal H_{II} coil inside	inverted cubic (bcc) C_I rod inside	cubic C_{II} coil inside
c_1	1	$2\sqrt{f}$	$2\sqrt{1-f}$	$3f^{2/3}$	$3(1-f)^{2/3}$
c_2	$\frac{\pi^2}{8}(1-f)$	$\frac{\pi^2}{16}\frac{(1-\sqrt{f})^3(3+\sqrt{f})}{(1-f)^2}$	$\frac{\pi^2}{16}$	$\frac{3\pi^2}{80}\frac{(1-f^{1/3})^3(6+3f^{1/3}+f^{2/3})}{(1-f)^2}$	$\frac{3\pi^2}{80}(1-f)^{-1/3}$

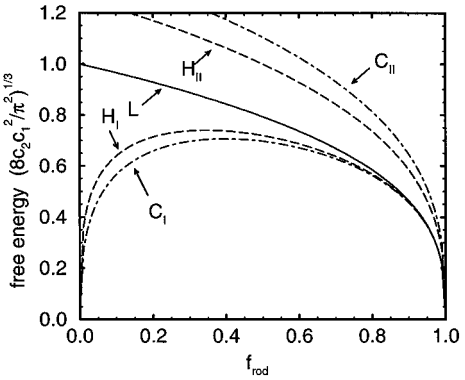

Figure 2. Free energies in the strong stretching approximation. Note that the free energies of the lamellar, hexagonal, and cubic phases are proportional. Packing constraints for the cubic phase are not taken into account.

energy of the nonlamellar phases. The ratios of the free energy of the normal (coil inside) hexagonal and cubic phase to the lamellar phase are independent of composition, f, and are $2^{1/3}$ and $2.7^{1/3}$, respectively. Therefore, we do not expect these phases to become stable in the strong segregation limit. Furthermore, the lower bound of the free energy of the inverted (coil outside) hexagonal phase is always lower than the free energy of the lamellar phase which would indicate that the lamellar phase is never stable in this limit. However an upper bound of the free energy of the hexagonal phases can be obtained[18] using concentric, hexagonal cylinders for the rod- and coil-rich region. As for flexible copolymers, this increases the free energy by about a factor of $(10/9)^{1/3}$. Comparison of this upper bound with the free energy of the lamellar phase indicates that the lamellar phase does become stable for $f > 0.765$ and large incompatibilities.

Thus far we have assumed that the rigid part of the copolymer packs space without free energy costs. In the lamellar and inverted hexagonal morphology, this is always possible by tilting the rods parallel to the rod−coil interface. The degree of alignment is characterized by the ratio of the size of the unit cell, R_{opt}, to the rod length, fNb. A convenient measure of this ratio is the parameter[10]

$$\kappa = \left(\frac{a^2}{3b^3\rho_0}\frac{\gamma}{N}\right)^{1/3} = \left(\frac{2c_2f^3}{3c_1}\right)^{1/3}\frac{R_{opt}}{fNb} \qquad (3.3)$$

which is defined so as to be explicitly independent of the rod fraction f. Since the chains are not completely extended, $\kappa \ll 1$. In the hexagonal phase, the rods are aligned predominantly along the cylinder axis, and the angle between the rods and this axis is on the order of κ. In the lamellar phase the rods are aligned predominantly parallel to the lamellae, and the angle between the rods and the normal to the lamellae differs from $\pi/2$ by the order of κ. As κ is so small, the rodlike parts are strongly oriented. In the cubic phase of spherical micelles, the size of the rod-rich spheres must be larger than the rod length, so that $2f^{1/3}R_{opt} > fNb$. This yields the following condition for the stability of the cubic phase with respect to the hexagonal one:

$$\kappa > \left(\frac{\pi^2 f^{4/3}(1-f^{1/3})^3(6+3f^{1/3}+f^{2/3})}{960(1-f)^2}\right)^{1/3} \qquad (3.4)$$

Since $\kappa \ll 1$, this condition for the stability of the cubic phase can only be met for very small values of f.

If our model included anisotropic interactions, which can be modeled by a quadrupolar Maier−Saupe form,[13,15] we would expect the stability region of the cubic phase to be reduced markedly or even to vanish completely, due to pronounced problems in packing rods into spheres. The effect of such interactions on the transition between the lamellar and the hexagonal phase is less clear. Such interactions would decrease the orientational entropy, which in the absence of such interactions is larger in the lamellar phase than in the hexagonal one. They would also increase the surface tension. Both of these effects tend to stabilize the hexagonal phase with respect to the lamellar one.

IV. Discussion

The extreme conformational asymmetry in rod−coil diblock copolymers has a pronounced influence on the phase behavior of these composite materials. Both the numerical self-consistent field theory in the weak segregation limit and the strong segregation theory at high incompatibilities predict that only morphologies in which the coils are on the convex side of the interface are thermodynamically stable. Differences in the phase behavior of this system and that of structurally symmetric coil−coil copolymers stem mainly from the lack of entropy in the rigid rod.

The phase behavior we have obtained is in qualitative agreement with recent experiments by Stupp[21] and coworkers, who observed hexagonal and lamellar phases in *thin films* of rod−coil diblock molecules by TEM. These experiments on films find the transition between the hexagonal and the lamellar phases to occur at lower rod contents f than do we for bulk. Besides effects of preferential absorption of one component to the surface of the film, and the neglect of anisotropic interaction in our model, this shift in the composition at the transition might be qualitatively accounted for by a simple packing argument. If the film thickness D is smaller than the rod length fNb, the size of the unit cell of the hexagonal phase must be minimized with the constraint $4fR^2 > (fNb)^2 - D^2 = R_{min}^2$. This yields for the ratio of the free energies of the hexagonal and lamellar phases:

$$\frac{F_H}{F_L} = \left(\frac{2048}{9}\right)^{1/3}\kappa\frac{f}{(1-f)^{1/3}\sqrt{f^2-x^2}} + \frac{1}{24(12\kappa)^{2/3}}(f^2-x^2)\frac{(1-\sqrt{f})^3(3+\sqrt{f})}{f(1-f)^{7/3}} \qquad (4.1)$$

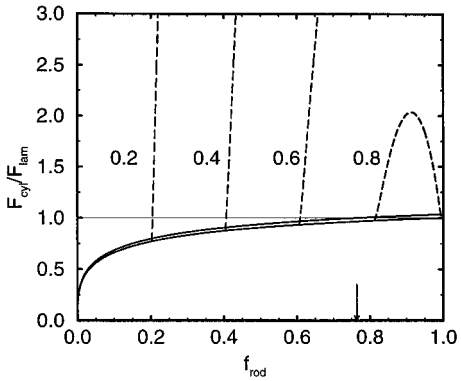

Figure 3. Influence of a confined geometry: ratio of the free energy of the HEX I phase and the LAM phase for $x = D/Nb = 0.2$, 0.4, 0.6, and 0.8, $\kappa = 0.01$. The solid lines are upper and lower bounds to the free energy of the bulk HEX I phase. The arrow indicates the composition beyond which a bulk lamellar phase might become stable.

where $x = D/Nb$ denotes the film thickness in units of the rod length. This ratio is shown in Figure 3 for different values of film thickness x and $\kappa = 0.01$. As one increases the film thickness, the transition between the hexagonal and lamellar phases is shifted to larger fractions of the rod, f. This effect is observed in experiment.[21]

Acknowledgment. Financial support by the Alexander von Humboldt foundation and the National Science Foundation under Grant No. DMR9531161 are gratefully acknowledged.

References and Notes

(1) Semenov, A. N. Sov Phys. JETP **1985**, *61*, 733. Likhtman, A. E.; Semenov, A. N. *Macromolecules* **1987**, *27*, 3103.

(2) van Berkel, R. W. M.; de Graaf, S. A. F.; Huntjens, F. J.; Vrouenraets, C. M. F. *Developments in Block Copolymers-1*; Goodman, I., Ed.; Applied Science Publishers: New York, 1982; p 261.

(3) Chen, J. T.; Thomas, E. L.; Zimba, C. G.; Rabolt, J. F. *Macromolecules* **1995**, *28*, 5811.

(4) Baker, G. L.; Bates, F. S. *Macromolecules* **1987**, *17*, 2619.

(5) Saunders, R. S.; Cohen, R. E.; Schrock, R. R. *Macromolecules* **1991**, *24*, 5599.

(6) Khoklov, A. R.; Semenov, A. N. *Physica* **1981**, *108A*, 546.

(7) Brochard, F.; Jouffry, J.; Levinson, P. *J. Phys. (Paris)* **1984**, *45*, 1125.

(8) ten Bosch, A.; Pinton, J. F.; Maissa, P.; Sixou, P. *J. Phys.* **1987**, *A20*, 4531.

(9) Liu, A. J.; Fredrickson, G. H. *Macromolecules* **1993**, *26*, 2817.

(10) Semenov, A. N.; Vasilenko, S. V. *Sov. Phys. JETP* **1986**, *63*, 70.

(11) Halperin, A. *Euro. Phys. Lett.* **1989**, *10*, 549.

(12) Williams, D. R. M.; Fredrickson, G. H. *Macromolecules* **1992**, *25*, 3561.

(13) Hołyst, R.; Schick, M. *J. Chem. Phys.* **1992**, *96*, 721: Singh, C.; Goulian, M.; Liu, A. J.; Fredrickson, G. H. *Macromolecules* **1994**, *27*, 2974.

(14) Matsen, M. W. *J. Chem. Phys.* **1996**, *104*, 7758.

(15) Netz, R. R.; Schick, M. *Phys. Rev. Lett.* **1996**, *77*, 302.

(16) Szleifer, I.; Ben-Shaul, A.; Gelbart, W. M. J. *Chem. Phys.* **1986**, *85*, 5345; ibid **1987**, *86*, 7094.

(17) Matsen, M. W.; Schick, M. *Phys. Rev. Lett.* **1994**, *72*, 2660.

(18) Olmsted, P. D.; Milner, S. T. *Phys. Rev. Lett.* **1994**, *72*, 936: Milner, S. T. J. Polym. Sci. **1994**, *B 32*, 2743.

(19) The orientational entropy loss per chain is smaller than the interfacial or stretching contribution in the strong segregation limit.

(20) Matsen, M. W.; Bates, F. S. *Macromolecules* **1995**, *28*, 8884.

(21) Radzilowiski, L. H.; Stupp, S. I. *Macromolecules* **1994**, *27*, 7747.

MA960782+